ORGANIC LETTERS

2013
Vol. 15, No. 12
3154–3157

Fluorescence Photoactivation by Ligand Exchange around the Boron Center of a BODIPY Chromophore

Sherif Shaban Ragab, Subramani Swaminathan, Erhan Deniz, Burjor Captain, and Françisco M. Raymo*

Laboratory for Molecular Photonics, Department of Chemistry, University of Miami, 1301 Memorial Drive, Coral Gables, Florida 33146-0431, United States

fraymo@miami.edu

Received May 16, 2013

ABSTRACT

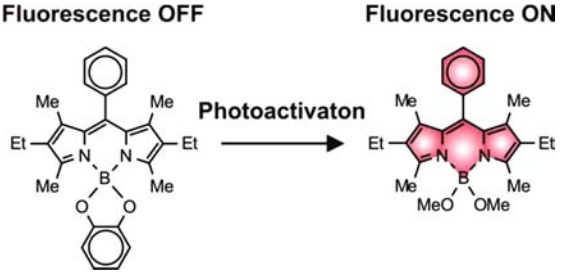

Chelation of the boron center of the borondipyrromethene (BODIPY) platform by a catecholate ligand results in effective fluorescence suppression. Electron transfer from the chelating unit to the adjacent chromophore upon excitation is responsible for fluorescence quenching. Under the influence of a photoacid generator, the catecholate chelator can be exchanged with a pair of methoxide ligands. This photoinduced transformation prevents electron transfer and efficiently activates the fluorescence of the BODIPY chromophore.

The ability to activate fluorescence under optical control offers the opportunity to monitor dynamic processes in real time.[1−5] Indeed, the illumination of a sample, labeled with a photoactivatable fluorophore, at an appropriate activating wavelength can switch fluorescence on exclusively within the irradiated area. After activation, fluorescence images can be recorded sequentially to follow the spatial redistribution of the fluorescent species and extract quantitative information on their diffusion. This protocol is conceptually related to fluorescence recovery after photobleaching[6] (FRAP) and has been exploited successfully to probe the diffusion of molecules in biological specimens as well as to monitor the flow of liquids in microstructured channels. However, the implementation of FRAP schemes demands relatively high irradiation intensities to bleach the fluorescent species and turn their emission off. Instead, photoactivatable fluorophores can be switched on with moderate activation intensities and, therefore, are a valuable alternative to FRAP in the investigation of dynamics at the microscopic level.

The unique combination of photochemical and photophysical properties of photoactivatable fluorophores can also be exploited to overcome the limitations that diffraction imposes on the resolving power of fluorescence microscopes.[7−12] Indeed, this fundamental physical phenomenon prevents the distinction of emissive species separated by subwavelength distances and restricts the spatial resolution of fluorescence images, recorded with visible light, to hundreds of nanometers. Instead, distinct photoactivatable fluorophores

(1) Adams, S. R.; Tsien, R. Y. *Annu. Rev. Physiol.* **1993**, *55*, 755–784.
(2) Politz, J. C. *Trends Cell Biol.* **1999**, *9*, 284–287.
(3) Dirks, R. W.; Molenaar, C.; Tanke, H. J. *Histochem. Cell Biol.* **2001**, *115*, 3–11.
(4) Ellis-Davies, G. C. *Nat. Methods* **2007**, *4*, 619–628.
(5) Xu, Y.; Melia, T. J.; Toomre, D. T. *Curr. Opin. Chem. Biol.* **2011**, *15*, 822–830.
(6) Ishikawa-Ankerhold, H. C.; Ankerhold, R.; Drummen, G. P. C. *Molecules* **2012**, *17*, 4047–4132.
(7) Huang, B.; Bates, M.; Zhuang, X. *Annu. Rev. Biochem.* **2009**, *78*, 993–1016.
(8) Hell, S. W. *Nat. Methods* **2009**, *6*, 24–32.
(9) van de Linde, S.; Heilemann, M.; Sauer, M. *Annu. Rev. Phys. Chem.* **2012**, *63*, 519–540.
(10) Ha, T.; Tinnefeld, P. *Annu. Rev. Phys. Chem.* **2012**, *63*, 595–617.
(11) Moerner, W. E. *J. Microsc.* **2012**, *246*, 213–220.
(12) Raymo, F. M. *J. Phys. Chem. Lett.* **2012**, *3*, 2379–2385.

10.1021/ol401380n
Published on Web 06/05/2013

can be localized individually, even when they are closely spaced, simply by turning their emission on at different intervals of time. Under these conditions, the sequential acquisition of images permits the mapping of multiple emissive species with spatial resolution at the nanometer level. In fact, biological samples tagged with photoactivatable labels can be visualized with a resolution that is otherwise impossible to achieve with conventional fluorophores.

The prospects of monitoring dynamics and overcoming diffraction are stimulating the design of mechanisms to photoactivate fluorescence with the main families of organic fluorophores.[13−18] Generally, these operating principles rely on either the photoinduced cleavage of a protecting group from an emissive chromophore or a photochromic transformation. In both instances, significant fluorescence is observed only after the formation of the photochemical product. Indeed, several examples of photoactivatable coumarins,[19−22] fluoresceins,[23−30] and rhodamines[29,31−34] have been developed already on the basis of these mechanisms. By contrast, only two strategies to photoactivate the emission of the BODIPY chromophore have been reported so far and they are both based on the photoinduced cleavage of 2-nitrobenzyl quenchers.[35,36] The BODIPY skeleton, however, offers outstanding photophysical properties together with synthetic accessibility.[37−40] Therefore, the identification of structural designs to activate the fluorescence of this versatile organic chromophore can translate into the realization of valuable photoactivatable probes for a diversity of imaging applications.

Table 1. Absorption (λ_{Ab}) and Emission (λ_{Em}) Wavelengths As Well As Fluorescence Quantum Yields (ϕ) of **1**−**3** in MeCN at 25 °C[a]

	λ_{Ab} (nm)	λ_{Em} (nm)	ϕ
1	521	536	0.66
2	523	536	0.30
3	527	—	—

[a] The corresponding absorption and emission spectra are reported in the Supporting Information (Figures S1−S3).

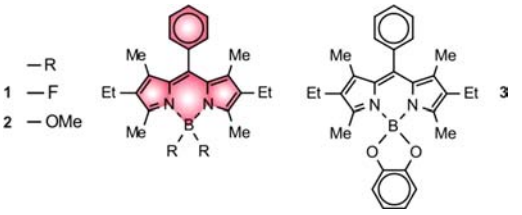

Spectroscopic data from our[41] and other[42] laboratories demonstrate that the replacement of the two fluorine ligands on the boron center of the BODIPY platform with a catecholate chelator suppresses fluorescence completely. These observations suggest that the manipulation of the groups attached to this particular atom can be exploited to regulate the emissive behavior of the overall chromophore and, possibly, activate fluorescence under optical control. Indeed, this letter reports the implementation of a mechanism for fluorescence activation based on the photoinduced exchange of the ligands connected to the BODIPY fluorophore.

The absorption and emission spectra (Figure S1) of **1** show the characteristic bands of the BODIPY chromophore at 521 and 536 nm (λ_{Ab} and λ_{Em} in Table 1) respectively in acetonitrile with a fluorescence quantum yield (ϕ in Table 1) of 0.66 in agreement with literature data.[43] Treatment of this compound with sodium methoxide results in the displacement of the two fluoride ligands around the boron center with the formation of **2**.[44] This structural transformation has negligible influence on λ_{Ab} and λ_{Em} (Table 1 and Figure S2), but lowers ϕ to 0.30.

Reaction of **1** with catechol, in the presence of aluminum chloride, also results in the displacement of the fluoride

(13) Mitchison, T. J.; Sawin, K. E.; Theriot, J. A.; Gee, K.; Mallavarapu, A. *Methods Enzymol.* **1998**, *291*, 63–78.
(14) Wysocki, L. M.; Davis, L. D. *Curr. Opin. Chem. Biol.* **2011**, *15*, 752–759.
(15) Puliti, D.; Warther, D.; Orange, C.; Specht, A.; Goeldner, M. *Bioorg. Med. Chem.* **2011**, *19*, 1023–1029.
(16) Raymo, F. M. *ISRN Phys. Chem.* **2012**, 619251–1−15.
(17) Li, W.-H.; Zheng, G. *Photochem. Photobiol. Sci.* **2012**, *11*, 460–471.
(18) Klán, P.; Šolomek, T.; Bochet, C. G.; Blanc, A.; Givens, R.; Rubina, M.; Popik, V.; Kostikov, A.; Wirz, J. *Chem. Rev.* **2013**, *113*, 119–191.
(19) Orange, C.; Specht, A.; Puliti, D.; Sakr, E.; Furuta, T.; Winsor, B.; Goeldner, M. *Chem. Commun.* **2008**, 1217–1219.
(20) Gagey, N.; Emond, M.; Neveu, P.; Benbrahim, C.; Goetz, B.; Aujard, I.; Baudin, J.-B.; Jullien, L. *Org. Lett.* **2008**, *10*, 2341–2344.
(21) Zheng, G.; Cochella, L.; Liu, J.; Hobert, O.; Li, W.-H. *ACS Chem. Biol.* **2011**, *6*, 1332–1338.
(22) Deniz, E.; Tomasulo, M.; Cusido, J.; Yildiz, I.; Petriella, M.; Bossi, M. L.; Sortino, S.; Raymo, F. M. *J. Phys. Chem. C* **2012**, *116*, 6058–6068.
(23) Krafft, G. A.; Sutton, W. R.; Cummings, R. T. *J. Am. Chem. Soc.* **1988**, *110*, 301–303.
(24) Mitchison, T. J. *J. Cell Biol.* **1989**, *109*, 637–652.
(25) Vincent, J. P.; O'Farrell, P. H. *Cell* **1992**, *68*, 923–931.
(26) Pellois, J.-P.; Hahn, M. E.; Muir, T. W. *J. Am. Chem. Soc.* **2004**, *126*, 7170–7071.
(27) Kobayashi, T.; Urano, Y.; Kamiya, M.; Ueno, T.; Kojima, H.; Nagano, T. *J. Am. Chem. Soc.* **2007**, *129*, 6696–6697.
(28) Zheng, G.; Guo, Y.-M.; Li, W.-H. *J. Am. Chem. Soc.* **2007**, *129*, 10616–10617.
(29) Maurel, D.; Banala, S.; Laroche, T.; Johnsson, K. *ACS Chem. Biol.* **2010**, *5*, 507–516.
(30) Yuan, L.; Lin, W.; Cao, Z.; Long, L.; Song, J. *Chem.—Eur. J.* **2011**, *17*, 689–696.
(31) Ottl, J.; Gabriel, D.; Marriott, G. *Bioconjugate Chem.* **1998**, *9*, 143–151.
(32) Gee, K. R.; Weinberg, E. S.; Kozlowski, D. J. *Bioorg. Med. Chem. Lett.* **2001**, *11*, 2181–2183.
(33) Belov, V. N.; Bossi, M. L.; Fölling, J.; Boyarskiy, V. P.; Hell, S. W. *Chem.—Eur. J.* **2009**, *15*, 10762–10776.
(34) Wysocki, L. M.; Grimm, J. B.; Tkachuk, A. N.; Brown, T. A.; Betzig, E.; Lavis, L. D. *Angew. Chem., Int. Ed.* **2011**, *50*, 11206–11209.
(35) Kobayashi, T.; Komatsu, T.; Kamiya, M.; Campos, C.; González-Gaitán, M.; Terai, T.; Hanaoka, K.; Nagano, T.; Urano, Y. *J. Am. Chem. Soc.* **2012**, *134*, 11153–11160.
(36) Shaban Ragab, S.; Swaminathan, S.; Baker, J. D.; Raymo, F. M. *Phys. Chem. Chem. Phys.*, DOI: 10.1039/c3cp51580j.
(37) (a) Loudet, A.; Burgess, K. *Chem. Rev.* **2007**, *107*, 4891–4932. (b) Kamkaew, A.; Lim, S. H.; Lee, H. B.; Kiew, L. V.; Chung, L. Y.; Burgess, K. *Chem. Soc. Rev.* **2013**, *42*, 77–88.
(38) (a) Ziessel, R.; Ulrich, G.; Harriman, A. *New J. Chem.* **2007**, *31*, 496–501. (b) Ulrich, G.; Ziessel, R.; Harriman, A. *Angew. Chem., Int. Ed.* **2008**, *47*, 1184–1201.
(39) Benstead, M.; Mehl, G. H.; Boyle, R. W. *Tetrahedron* **2011**, *67*, 3573–3601.
(40) Boens, N.; Leen, V.; Dehaen, W. *Chem. Soc. Rev.* **2012**, *41*, 1130–1172.
(41) Deniz, E.; Battal, M.; Cusido, J.; Sortino, S.; Raymo, F. M. *Phys. Chem. Chem. Phys.* **2012**, *14*, 10300–10307.
(42) Tahtaoui, C.; Thomas, C.; Rohmer, F.; Klotz, P.; Duportail, G.; Mely, Y.; Bonnet, D.; Hibert, M. *J. Org. Chem.* **2007**, *72*, 269–272.
(43) Gabe, Y.; Urano, Y.; Kikuchi, K.; Kojima, H.; Nagano, T. *J. Am. Chem. Soc.* **2004**, *126*, 3357–3367.
(44) Lundrigan, T.; Crawford, S. M.; Cameron, T. S.; Thompson, A. *Chem. Commun.* **2012**, *48*, 1003–1005.

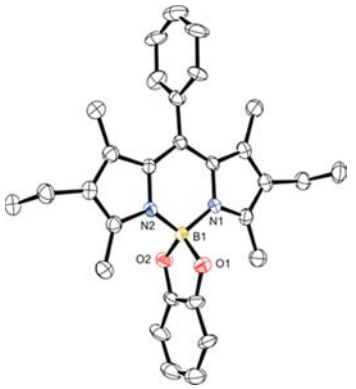

Figure 1. ORTEP representation of the geometry adopted by **3** in single crystals, showing 50% thermal ellipsoid probability.

ligands around the boron center of the BODIPY platform to produce **3**.[41] X-ray diffraction analysis (Table S1) of single crystals of the product reveals the tetrahedral geometry of this particular atom with the coordination of a single catecholate chelator (Figure 1). The exchange of the ligands has, once again, negligible influence on λ_{Ab} (Table 1 and Figure S3), but completely suppresses the emission of the BODIPY chromophore. Presumably, the transfer of one electron from the catecholate chelator to the adjacent BODIPY platform, upon excitation, is responsible for fluorescence quenching. Indeed, time-dependent density-functional theory (TDDFT) supports this interpretation of the excitation dynamics of **3**. Specifically, TDDFT calculations with two different functionals (B3LYP and MPW1PW91), in combination with the 6-311+G(d,p) basis set and a solvation model for acetonitrile, assign the main absorption band of **2** and **3** in the visible region to the population of the first singlet excited state (S_1). The estimated excitation energy is *ca.* 2.7 eV (ΔE in Table S2) with an oscillator strength of *ca.* 0.6 (*f* in Table S2).[45] The occupied and unoccupied molecular orbitals mainly responsible for this electronic transition are both centered on the BODIPY chromophore (Figure S4). In addition, these calculations indicate the existence of an intramolecular charge-transfer (ICT) state exclusively in the case of **3**. This state is positioned *ca.* 2.4 eV (Table S2) above the ground state (S_0) and its population involves the formal transfer of one electron from an occupied molecular orbital, localized on the catecholate ligand (Figure S4), to an unoccupied molecular orbital, centered on the BODIPY platform. The ICT state of **3** is essentially forbidden, but it can be accessed from S_1 after excitation (Figure 2). As a result, its presence provides a nonradiative pathway for the deactivation

(45) TDDFT calculations are known to overestimate the excitation energy of BODIPY chromophores (Nithya, R.; Kolandaivel, P.; Senthilkumar, K. *Mol. Phys.* **2012**, *110*, 445–456). In fact, the absorption spectra of **2** and **3** (Figures S2 and S3) indicate the excitation energy to be *ca.* 2.4 eV for both compounds. This experimental value is *ca.* 0.3 eV lower than those calculated for **2** and **3** (Table S2) with the B3LYP and MPW1PW91 functionals at the 6-311+G(d,p) level.

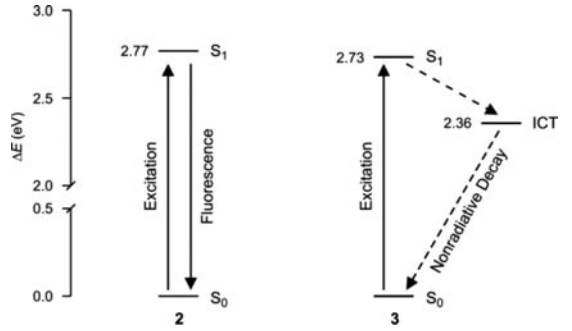

Figure 2. Excitation dynamics of **2** and **3** with B3LYP energies of the associated electronic states.

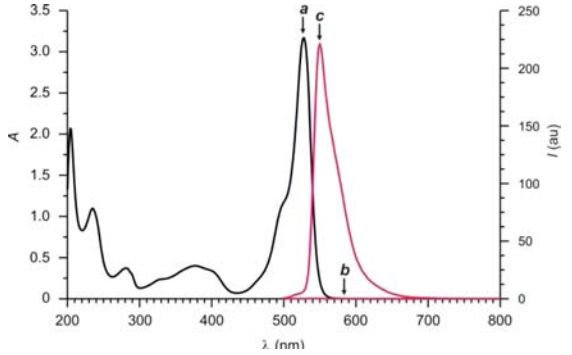

Figure 3. Absorption spectrum (a) of a MeOH solution (100 μM, 25 °C) of **3**. Emission spectra (λ_{Ex} = 490 nm) of a MeOH solution (10 μM, 25 °C) of **3**, recorded before (b) and after (c) the addition of TFA (1 equiv).

of the excited state that is otherwise responsible for the fluorescence of the BODIPY chromophore. Such a pathway is not available in **2**, and in fact, this compound reverts radiatively to S_0 after excitation to S_1 (Figure 2).

The spectroscopic behavior of **3** in methanol parallels that observed in acetonitrile. In particular, the absorption spectrum (spectrum a in Figure 3) shows the characteristic band of the BODIPY chromophore at a λ_{Ab} of 528 nm, while the emission spectrum (spectrum b in Figure 3) does not reveal any significant fluorescence. Upon addition of 1 equiv of trifluoroacetic acid (TFA), however, an intense band appears at a λ_{Em} of 550 nm (spectrum c in Figure 3).[46] By contrast, the very same treatment in acetonitrile does not cause any change to the emission spectrum. These observations suggest that the catecholate chelator of the nonemissive species **3** is replaced by two methoxide ligands to form the emissive BODIPY **2**, under acidic conditions in methanol. Indeed, the electrospray ionization mass spectra, recorded before and after this treatment, show the appearance of a peak for the molecular ion of **2**, upon

(46) The addition of TFA has negligible influence on the absorption spectrum in methanol as well as in acetonitrile.

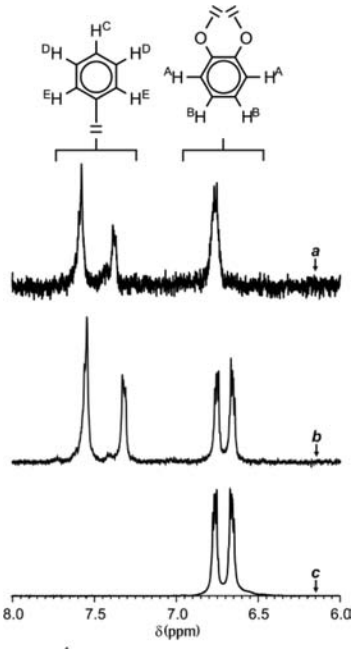

Figure 4. Partial ^{1}H NMR spectra (400 MHz) of CD_3OD solutions (10 mM, 25 °C) of **3**, recorded before (a) and after (b) the addition of TFA (1 equiv), and of catechol (c).

acidification. Similarly, the ^{1}H nuclear magnetic resonance (NMR) spectra, recorded before and after the addition of acid in deuterated methanol, are also consistent with the transformation of **3** into **2**. In particular, the initial spectrum (spectrum a in Figure 4) shows a resonance centered at 6.75 ppm for the two pairs of homotopic protons (H^A and H^B) on the catecholate chelator of **3**. After acidification, this resonance splits into two sets of peaks centered at 6.74 and 6.66 ppm respectively (spectrum b in Figure 4). The very same peaks are also observed in the spectrum (spectrum c in Figure 4) of catechol, recorded under otherwise identical conditions. Instead, the resonances associated with the three sets of protons (H^C, H^D, and H^E) on the phenyl ring, attached to the *meso* position of the BODIPY chromophore, remain essentially unaffected with the addition of acid (spectra a and b in Figure 4).

The exchange of the catecholate chelator of **3** with the two methoxide ligands of **2** can be achieved also under optical control with the aid of a photoacid generator. Specifically, the ultraviolet illumination of **4** (Figure 5) is known to encourage the release of hydrogen bromide with the concomitant formation of **5**.[47] In turn, the photogenerated acid can promote the transformation of **3** into **2** in the presence of methanol. Indeed, the absorption spectra (spectrum a in Figure 5), recorded at regular intervals of time during the irradiation of an equimolar mixture of **3** and **4** in methanol, reveal the characteristic increase in absorbance at *ca.* 370 nm associated with the photoinduced

(47) Swaminathan, S.; Petriella, M.; Deniz, E.; Cusido, J.; Baker, J. D.; Bossi, M. L.; Raymo, F. M. *J. Phys. Chem. A* **2012**, *116*, 9928–9933.

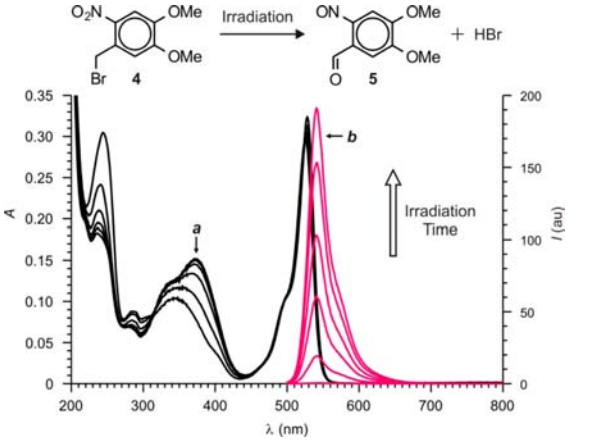

Figure 5. Absorption (a) and emission (b) spectra of equimolar MeOH solutions (10 μM, 25 °C, λ_{Ex} = 490 nm) of **3** and **4**, recorded before and during irradiation (300−410 nm, 3.33 mW cm^{-2}, 5 min) with intervals of 1 min.

formation of **5**. Instead, the absorption band in the visible region remains essentially unaffected, demonstrating that the BODIPY chromophore tolerates these irradiation conditions. In agreement with the formation of **5** and the concomitant release of acid, the corresponding emission spectra (spectrum b in Figure 5) show the growth of a band for the photogenerated fluorophore **2**. By contrast, no fluorescence can be detected under irradiation of **3** in the absence of **4**, under otherwise identical conditions, confirming that the photoacid generator is essential to activate emission.

These results demonstrate that the manipulation of the ligands around the boron center of the BODIPY platform can be exploited to activate emission under optical control. Indeed, the photoinduced generation of acid can mediate the exchange of a catecholate chelator with a pair of methoxide ligands and suppress the electron-transfer pathway that would otherwise be responsible for fluorescence quenching. Thus, these operating principles for fluorescence activation, coupled to the synthetic versatility of BODIPY chromophores and their outstanding photochemical and photophysical properties, can eventually lead to the development of valuable photoactivatable probes for a diversity of imaging applications.

Acknowledgment. The National Science Foundation (CAREER Award CHE-0237578, CHE-0749840, and CHE-1049860) is acknowledged for supporting our research program.

Supporting Information Available. Experimental procedures and computational protocol; absorption and emission spectra of **1**−**3** in MeCN; crystallographic data for **3**; computed excited states, molecular orbitals, and coordinates of **2** and **3**. This material is available free of charge via the Internet at http://pubs.acs.org.

The authors declare no competing financial interest.